

Intra-coronary Stent Localization in Intravascular Ultrasound Sequences, A Preliminary Study

Simone Balocco^{1,2(✉)}, Francesco Ciompi^{3,4}, Juan Rigla⁵, Xavier Carrillo⁶,
Josepa Mauri⁶, and Petia Radeva^{1,2}

¹ Department Matematics and Informatics, University of Barcelona,
Gran Via 585, 08007 Barcelona, Spain
balocco.simone@gmail.com

² Computer Vision Center, 08193 Bellaterra, Spain

³ Computational Pathology Group, Department of Pathology,
Radboud University Medical Center, Nijmegen, Netherlands

⁴ Diagnostic Image Analysis Group, Department of Radiology
and Nuclear Medicine, Radboud University Medical Center, Nijmegen, Netherlands

⁵ InspireMD, Boston, MA, USA

⁶ University Hospital Germans Trias I Pujol, 08916 Badalona, Spain

Abstract. An intraluminal coronary stent is a metal scaffold deployed in a stenotic artery during Percutaneous Coronary Intervention (PCI). Intravascular Ultrasound (IVUS) is a catheter-based imaging technique generally used for assessing the correct placement of the stent. All the approaches proposed so far for the stent analysis only focused on the struts detection, while this paper proposes a novel approach to detect the boundaries and the position of the stent along the pullback. The pipeline of the method requires the identification of the stable frames of the sequence and the reliable detection of stent struts. Using this data, a measure of likelihood for a frame to contain a stent is computed. Then, a robust binary representation of the presence of the stent in the pullback is obtained applying an iterative and multi-scale approximation of the signal to symbols using the SAX algorithm. Results obtained comparing the automatic results versus the manual annotation of two observers on 80 IVUS in-vivo sequences shows that the method approaches the inter-observer variability scores.

1 Introduction

An intraluminal coronary stent is a metal mesh tube deployed in a stenotic artery during Percutaneous Coronary Intervention (PCI). Ideally, the stent should be implanted and optimally expanded along the vessel axis, considering vessel anatomical structures such as bifurcations and stenoses.

Intravascular Ultrasound (IVUS) is a catheter-based imaging technique generally used for assessing the correct expansion, aposition and precise placement

S. Balocco and F. Ciompi equally contributed to the paper.

© Springer International Publishing AG 2017

M.J. Cardoso et al. (Eds.): CVII-STENT/LABELS 2017, LNCS 10552, pp. 12–19, 2017.

DOI: 10.1007/978-3-319-67534-3_2

of the stent. The IVUS images can be visualized in long-axis view, allowing a pullback-wise analysis and in short axis view allowing a frame-wise analysis (see Fig. 1(a and b)). The physician examines both views, identifying the presence of struts. The analysis of a single short-axis image sometimes is not sufficient for accurately assessing if struts are present. In most of ambiguous cases, the physician has to scroll the pullback back and forward, analyzing adjacent frames until the stent boundaries are detected.

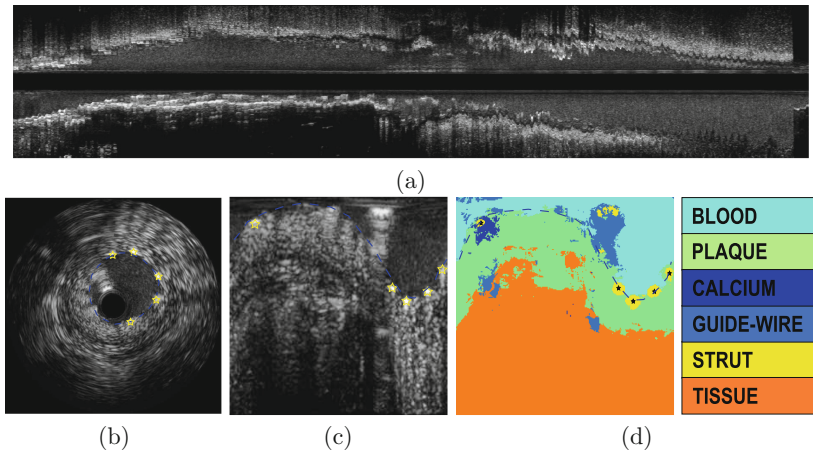


Fig. 1. Example of IVUS image in long axis view (a) and in short axis view (b, c). The IVUS image is represented in polar (b) and in cartesian (c) coordinates, along with the corresponding classification maps of the short-axis cartesian image (d). The detected struts are represented using a yellow (c) and black (d) star markers. The automatic stent shape is represented in dashed blue line. (Color figure online)

To date, all the approaches for automatic stent analysis in IVUS assume that the analyzed frame always contains a stent [1–5], and no strategies have been proposed so far for detecting the boundaries and the position of the stent along the pullback. Instead, this paper extends a previously published stent detection method [1] by identifying the presence (location and extension) of the stent along the pullback.

The pipeline of the framework requires the identification of the stable frames of the sequence using an image-based gating technique [6] and the reliable detection of stent struts [1]. Then, this paper introduces a measure of likelihood for a frame to contain a stent, which we call *stent presence*. A temporal series is obtained by computing such likelihood along the whole sequence. The mono-dimensional signal is modeled as a train of rectangular waves by using an iterative and multi-scale approximation of the signal to symbols using the SAX algorithm [7], which allows to obtain a robust binary representation of the presence of the stent in the pullback.

In order to extensively validate the proposed CAD system, we collected a set of 80 IVUS in-vivo sequences. The data sets includes about 700 IVUS images containing metallic stents.

2 Method

2.1 Gating

Let us define an IVUS pullback as a sequence of frames $I = \{f_i\}$ where i is the frame number of the sequence. In the proposed pipeline, we first pre-process the pullback by applying an image-based gating procedure. Gating is a necessary step in order to make the analysis robust to two kinds of artifacts generated by the heart beating: the *swinging* effect (repetitive oscillations of the catheter along the axis of the vessel) and the *roto-pulsation* effect (irregular displacement of the catheter along the direction perpendicular to the axis of the vessel). For this purpose, the method presented by Gatta et al. [6] is applied to the IVUS pullback, which selects a sequence of gated frames $G = \{f_{g_j}\}$ that are processed by the system.

2.2 Struts Detection

The detection of stent struts was performed by applying the Computer-Aided Detection (CAD) framework proposed by Ciompi et al. [1] to each gated frame independently. The method, provides a reliable identification of the stent struts, by contemporaneously considering the textural appearance of the stent and the vessel morphology. The CAD system uses the Multi-Scale Multi-Class Stacked Sequential Learning (M²SSL) classification scheme to provide a comprehensive interpretation of the local structure of the vessel. In the classification problem, the class *Strut* is considered as one of the six considered classes (defined as Blood area, Plaque, Calcium, Guide-wire shadow, Strut and external Tissues). For semantic classification purposes, tailored features used for classification to the problem [8] are used.

For each pixel $p(x, y)$ of a gated IVUS image, a classification map M is obtained (see Fig. 1(c)). A curve approximating the stent shape S_{shape} is initially estimated considering vascular constrains and classification results. For each region of M labelled as stent ($M_{\{S\}}$), a strut candidate is considered. The selected struts $p_s(x, y)$ were selected among the candidates, considering both local *appearance* and distance with respect to the stent shape S_{shape} . Consequently false positives candidates were discarded, and the regions containing a selected strut struts $M_{\{S\}}^*$ are a subset of $M_{\{S\}}$.

2.3 Stent Presence Assessment

The frames of the pullback corresponding to the vessel positions where the stent begins and ends can be identified by analyzing the detected struts. We model the

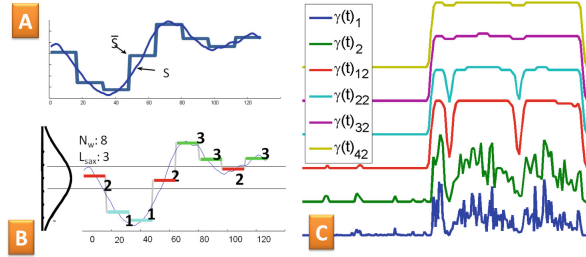


Fig. 2. Piecewise Aggregate Approximation of a generic signal (a) and quantization of $\gamma(t)$ after gaussian normalization (b). In (c) iterations of the SAX algorithm over an exemplar signal $\gamma(t)$ are illustrated.

presence of stent as a rectangular function $\Pi(t)$, where the variable t indicates the spatial position in the pullback. We estimate the binary signal $\Pi(t)$ by processing a real-valued signal $\gamma(t)$, which we define *stent presence*, corresponding to the frame-based likelihood of finding a stent in each frame of the IVUS sequence. The value of $\gamma(t)$ for each position t in the sequence is computed by considering both the number of struts and their area, thus negatively weights small struts areas of the images which have an high probability to be incorrect an detection. The function $\gamma(t)$ is defined as follows:

$$\gamma(t) = \sum_{p \in M_{\{S\}}^*} p |_{p_s \in M_{\{S\}}^*} \quad (1)$$

where $p_s \in M_{\{S\}}^*$ indicates the pixels of the IVUS frame labeled as *strut* containing an selected strut. An example of signal $\gamma(t)$ is depicted in Fig. 2(c).

The signal $\gamma(t)$ may contain several transitions between low and high amplitudes, due to the variability in the number of struts visible in consecutive frames and to suboptimal struts detection. For this reason, we filter the $\gamma(t)$ signal by considering its local statistics applying the SAX algorithm [7]. SAX is a symbolic representation algorithm that estimates a quantization of the time series based on global signal measurements and on local statistics of subsequent neighbor samples. Given the signal $\gamma(t)$ and a window size w , the algorithm calculates a Piecewise Aggregate Approximation (PAA) $\widehat{\gamma}(t)$, which is obtained by computing the local average values of $\gamma(t)$ over n_w segments w -wide. Each average value is then normalized over the signal $\gamma(t)$. The procedure firstly computes a vector $\bar{\gamma}(t) = (\bar{q}_1, \dots, \bar{q}_{n_w})$ where each of \bar{q}_i is calculated as follows:

$$\bar{q}_i = \frac{1}{w} \sum_{j=w(i-1)+1}^{w \cdot i} q_j, \quad (2)$$

where $i, j \in \mathbb{N}$. Then, considering a Gaussian distribution of the samples, the quantified values \hat{q}_i are obtained by normalizing \bar{q}_i by the mean μ_γ and standard deviation σ_γ of the signal $\gamma(t)$:

$$\hat{q}_i = \frac{\bar{q}_i - \mu_\gamma}{\sigma_\gamma} \quad (3)$$

In Fig. 2(a, b) a scheme illustrates how the PPA of a generic signal is computed by applying SAX. The values μ_γ and σ_γ of each $\gamma(t)$ are different, since the amplitude of $\gamma(t)$ is expected to be low in case of a pullback not containing a stent, and vice-versa. Therefore, in order to obtain a global estimation of such variables valid for any pullbacks, it is necessary to estimate mean and standard deviation over a training set consisting of a representative collection of stent pullbacks.

The SAX algorithm is iterated N_{sax} times, until converging to flat intervals along the signal $\gamma(t)$. Figure 2(c) illustrates the iteration of the SAX algorithm over an exemplar signal $\gamma(t)$. The maximum iteration number N_{sax} is achieved when the difference between subsequent iterations of SAX is zero. The other parameters of the SAX algorithm is the number of quantized values assigned to the signal L_{sax} . The iterative SAX algorithm is described by the following equation:

$$\gamma(t)_{k+1} = SAX(\gamma(t)_k, \sigma_k^{train_{sax}}, \mu_k^{train_{sax}}, L^{train_{sax}}) \quad (4)$$

where $k \in 1..N_{sax}$ and $\sigma_k^{train_{sax}}$ and $\mu_k^{train_{sax}}$ are the mean and standard deviation computed on the training set at the iteration k , and the number of quantized values L_{sax} is a constant that has been optimized using the training set. When the SAX algorithm reaches the maximum iteration number N_{sax} , the binary signal indicating the stent presence of the stent is obtained as $\square(t) = \gamma(t)_{N_{sax}} > \mu_{N_{sax}}^{train_{sax}}$.

3 Validation

3.1 Material

A set of 80 IVUS sequences containing a stent was collected. Roughly 50% of the frames contained a stent. The IVUS sequences were acquired using iLab echograph (Boston Scientific, Fremont, CA) with a 40 MHz catheter. The pullback speed was 0.5 mm/s.

Two experts (one clinician and one experienced researcher) manually annotated the beginning and the end of the stent in each sequence; more than one annotation per pullback was allowed when several stents were implanted in subsequent segments of the same artery.

3.2 Experiments on Stent Presence Assessment

The assessment of stent presence is based on the analysis of the mono-dimensional signal $\gamma(t)$. In order to evaluate the performance, the manual annotations of beginning and end of the stent were converted into binary signals $\gamma_{man}(t)$ indicating the presence of the stent in the pullback. Successively, the

signals $\square(t)$ indicating the segments of the pullback in which a stent is likely to be present, were compared against the sections indicated by the observers $\gamma_{man}(t)$. The performance were evaluated applying the algorithm to the sets $test_{met}$ and $test_{abs}$ and measures of *Precision* (P), *Recall* (R), *F-Measure* (F), and *Jaccard-index* (J) were considered.

In our experiments, we used the training set $train_{met}$ to estimate $\sigma_k^{train_{sax}}$, $\mu_k^{train_{sax}}$ and $L^{train_{sax}}$. The optimal number of quantized values assigned to the signal L_{sax} was chosen via cross-validation finding the value of $L_{sax} = 36$ as optimal.

Table 1. Quantitative evaluation the pullback analysis stage on both $test_{met}$ and $test_{abs}$ data-sets. For each data-set the performance of the automatic method versus each manual annotation are reported. Then the inter-observer variability is shown.

		Precision mean (std)	Recall mean (std)	F-measure mean (std)	Jaccard mean (std)
$test_{met}$	<i>auto vs obs-1</i>	85.4% (13.2%)	85.7% (7.7%)	84.8% (5.3%)	73.8% (13.7%)
	<i>auto vs obs-2</i>	89.5% (12.0%)	76.0% (10.6%)	80.7% (6.7%)	68.0% (13.8%)
	<i>obs-1 vs obs-2</i>	81.4% (11.3%)	98.8% (7.7%)	87.2% (7.8%)	80.7% (11.8%)

The quantitative results for the pullback-wise analysis is reported in Table 1. As IVUS is highly challenging to interpret, the two observers sometimes disagrees as shown Table 1. The precision approaches the inter-observer variability, while the recall is in general 10% lower than the results of the manual annotation. The obtained F-measure and the Jaccard measure of the automatic performance show satisfactory results when compared with manual annotations.

4 Results and Discussion

Examples of processed signals for the stent detection in IVUS frames are depicted in Fig. 3. In Fig. 3-(A1 and B1), both initial and final frame of the sequence are accurately identified. The result is not obvious since in (a) the amplitude of the signal $\gamma(t)$ is almost null in two sections of the pullback. However, the SAX algorithm allowed to detect the presence of stent, based on the statistics of the frames in the neighbourhood. On the other hand, in Fig. 3(A2), the central section of the pullback where $\gamma_{auto}(t)$ is almost null is correctly classified by the SAX algorithm as absence of stent. This is coherent with the manual annotation of the two observers, where two stents are labeled. In Fig. 3(B1 and B2), regions of high signal separated from the main stent have been identified as a secondary implanted stent. It might be noticed that this error happens only when strong spikes in the signal are present, for instance when a calcified plaque is mistaken for a deployed stent.

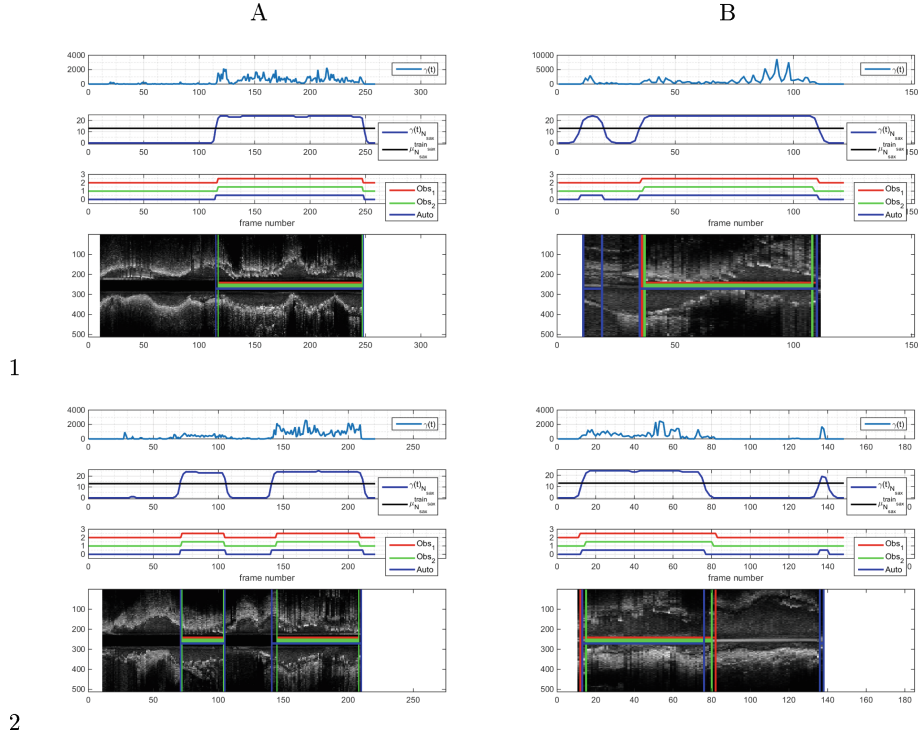


Fig. 3. Qualitative evaluation on $test_{met}$. The signal $\gamma(t)$ is illustrated in the first row, while in the second the result of the SAX quantization is reported. Finally in the third row, three binary signals representing the presence or the absence of the signal are compared: the first correspond to the automatic results, while the second and the third are the annotations of the two observers.

5 Conclusion

In this paper, a framework for the automatic identification of stent presence along the pullback (location and extension) has been presented. The analysis of the *stent presence* signal has been performed using the SAX algorithm with provides an unsupervised classification of the stent location in a fast and statistically robust fashion. The method has been implemented in Matlab and the computation time of the pullback analysis is about 4.1 s, one order of magnitude lower than the time required for detecting the stents [1] (33 s per pullback). Future work will be addressed towards validating the method with a larger data-set, including bio-absorbable stents.

Acknowledgments. This work was supported in part by the MICINN Grant TIN2015-66951-C2-1-R, SGR 1219, CERCA and ICREA Academia'2014.

References

1. Ciompi, F., Balocco, S., Rigla, J., Carrillo, X., Mauri, J., Radeva, P.: Computer-aided detection of intra-coronary stent in intravascular ultrasound sequences **43**(10), 5616–5625 (2016)
2. Canero, C., Pujol, O., Radeva, P., Toledo, R., Saludes, J., Gil, D., Villanueva, J., Mauri, J., Garcia, B., Gomez, J.: Optimal stent implantation: three-dimensional evaluation of the mutual position of stent and vessel via intracoronary echocardiography. In: *Computers in Cardiology*, pp. 261–264 (1999)
3. Dijkstra, J., Koning, G., Tuinenburg, J., Oemrawsingh, P., Reiber, J.: Automatic border detection in intravascular ultrasound images for quantitative measurements of the vessel, lumen and stent parameters. In: *Computers in Cardiology 2001*, vol. 28 (Cat. No. 01CH37287), vol. 1230, pp. 25–28 (2001)
4. Dijkstra, J., Koning, G., Tuinenburg, J.C., Oemrawsingh, P.V., Reiber, J.H.: Automatic stent border detection in intravascular ultrasound images. In: *International Congress Series*, vol. 1256, pp. 1111–1116. Elsevier (2003)
5. Rotger, D., Radeva, P., Bruining, N.: Automatic detection of bioabsorbable coronary stents in ivus images using a cascade of classifiers. *IEEE Trans. Inform. Technol. Biomed.* **14**, 535–537 (2010)
6. Gatta, C., Balocco, S., Ciompi, F., Hemetsberger, R., Leor, O.R., Radeva, P.: Real-time gating of IVUS sequences based on motion blur analysis: method and quantitative validation. In: Jiang, T., Navab, N., Pluim, J.P.W., Viergever, M.A. (eds.) *MICCAI 2010. LNCS*, vol. 6362, pp. 59–67. Springer, Heidelberg (2010). doi:[10.1007/978-3-642-15745-5_8](https://doi.org/10.1007/978-3-642-15745-5_8)
7. Lin, J., Keogh, E., Wei, L., Lonardi, S.: Experiencing sax: a novel symbolic representation of time series. *Data Min. Knowl. Disc.* **15**, 107 (2007)
8. Ciompi, F., Pujol, O., Gatta, C., Alberti, M., Balocco, S., Carrillo, X., Mauri-Ferre, J., Radeva, P.: Holimab: a holistic approach for media-adventitia border detection in intravascular ultrasounds. *Med. Image Anal.* **16**, 1085–1100 (2012)

Intravascular Imaging and Computer Assisted Stenting,
and Large-Scale Annotation of Biomedical Data and
Expert Label Synthesis

6th Joint International Workshops, CVII-STENT 2017 and
Second International Workshop, LABELS 2017, Held in
Conjunction with MICCAI 2017, Québec City, QC, Canada,
September 10-14, 2017, Proceedings

Cardoso, J.; Arbel, T.; Lee, S.-L.; Cheplygina, V.; Balocco,
S.; Mateus, D.; Zahnd, G.; Maier-Hein, L.; Demirci, S.;
Granger, E.; Duong, L.; Carbonneau, M.-A.; Albarqouni,
S.; Carneiro, G. (Eds.)

2017, XVI, 166 p. 73 illus., Softcover

ISBN: 978-3-319-67533-6